Published by Nigerian Society of Physical Sciences. Hosted by FLAYOO Publishing House LTD

Proceedings of the Nigerian Society of Physical Sciences

Journal Homepage: https://flayoophl.com/journals/index.php/pnspsc

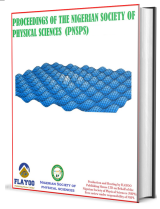

Influence of solution matrix on the adsorption capacity of NaOH-modified *Carica papaya* seed for Congo red and malachite green removal

Saheed Ademola Adesokan[a], Adetayo Damola Adelakin[b], Abdur-Rahim Adebisi Giwa[b,*], Deborah Olubunmi Aderibigbe[b]

[a]*Department of Industrial Chemistry, Abiola Ajimobi Technical University, 200255, Ibadan, Nigeria*
[b]*Department of Pure and Applied Chemistry, Ladoke Akintola University of Technology, PMB 4000, Ogbomoso, Nigeria*

ABSTRACT

Underutilized agro-based waste *Carica papaya* seed (CPS) was processed into a base-modified adsorbent for the remediation of malachite green (MG)- and Congo red (CR)-contaminated water. CPS was treated with 300 mL of 0.1 M NaOH for 24 h at room temperature, and the treated adsorbent was denoted as BCPS. BCPS was characterized using scanning electron microscopy (SEM), Fourier transform infrared (FTIR) spectroscopy and pH point of zero charge (pH_{pzc}). Batch adsorption studies were carried out as functions of contact time, adsorbent dose, solution pH, initial adsorbate concentration and temperature. Adsorption isotherm, kinetic and thermodynamic studies were also performed. FTIR analysis indicated surface groups including O–H, C≡C, C=C, C≡N, C–O, C–C and C–H; O–H, C=O, C≡N and C–H were implicated in MG and CR adsorption. The pH_{pzc} of BCPS was 6.2. BCPS showed higher adsorption capacity for MG than CR under most experimental conditions, except pH, where the optimum values for MG and CR adsorption were pH 9 and pH 3, respectively. Maximum adsorption capacities for MG in single and binary systems were 42.37 and 7.62 mg/g, respectively, whereas those for CR were 6.95 and 5.58 mg/g, respectively. Langmuir and pseudo-second-order models best described the isotherm and kinetic data, respectively, and the adsorption processes were thermodynamically feasible.

Keywords: Base-modified adsorbent, *Carica papaya* seed, Adsorbate molecular mass, Dye adsorption.

DOI:10.61298/pnspsc.2026.3.279

1. INTRODUCTION

Water is an indispensable finite resource. However, advances in virtually all areas of materials science have placed further pressure on water availability. Discharges from materials processing pollute the environment, including water. Pollutants find their way into natural freshwater, marine water, rainwater and groundwater sources [1].

These pollutants are of organic and inorganic origin and arise from industrial processes, agricultural applications, medical and pharmaceutical facilities, mining and metal smelting, domestic disposal, improper waste management, and textile and dyeing activities. Dyes in the environment affect water through coloration and toxic substances [2].

Malachite green (MG) and Congo red (CR) are two acidic/basic dye candidates used in a wide range of applications. Their presence in water is associated with carcinogenic tendency, coloration, reduced light penetration in aquatic systems, oxidative stress in aquatic organisms, bioaccumulation, teratogenicity,

*Corresponding Author Tel. No.: +234-803-5065-456
e-mail: giwa1010@gmail.com (Abdur-Rahim Adebisi Giwa)

mutagenicity and aesthetic degradation, among other effects [3].

Several technologies have been adopted for treating dye-polluted water, including ozonation, filtration, ultrafiltration, reverse osmosis, digestion, bioremediation and adsorption. These methods can be expensive, and some generate secondary substances that are more toxic or as toxic as the primary pollutants. Adsorption is relatively cheaper and efficient in water and wastewater treatment [4].

Conventional commercial adsorbents used in adsorption processes for water-treatment operations are expensive. To make adsorption cheaper, researchers have focused on developing new materials that are efficient, environmentally benign and economically attractive. Agricultural wastes are abundant, available for further processing and environmentally compliant. *Carica papaya* seed is one such abundant agricultural by-product in Nigeria. Nigeria is the fourth-largest producer of *Carica papaya* in the world, producing more than 800,000 metric tons per year [5]. This huge volume of seed ends up as waste.

The goals of developing new adsorbent materials for water treatment include process affordability, efficiency, selectivity, regenerability, robustness and ruggedness. Development of selective adsorbents may require understanding the relationships among the physicochemical properties of the adsorbent, the adsorbate and the adsorption-process parameters [6–8].

Carica papaya seeds are abundant agro-wastes with few known uses in this locality. This study was therefore conducted to convert *Carica papaya* seed into an adsorbent for the treatment of MG- and CR-contaminated water and to determine the influence of physicochemical parameters on its adsorptive capacity.

2. MATERIALS AND METHODS

2.1. MATERIALS

The materials used included *Carica papaya* seeds, NaOH, malachite green (MG; color index: 42000; lot no.: 130510; λ_{max}: 616 nm; molecular weight: 364.91 g/mol), supplied by Kem Light Laboratory, Mumbai, India, Congo red dye (CR; CAS: 573-58-0; λ_{max}: 496 nm; molecular weight: 696.66 g/mol), supplied by Timstar Laboratory Suppliers Ltd., Green Lane, Wardle, Nantwich, England, and distilled water. The equipment used included a pH meter, wet thermally regulated shaker, scanning electron microscope, transmission electron microscope, Fourier transform infrared spectrophotometer, UV–Vis spectrophotometer and laboratory apparatus.

2.1.1. Structures of MG and CR

The structures of CR and MG are presented in Figure 1. The nucleophilic and electrophilic centers are shown. CR has larger molecular length and surface area than MG. The implications of these parameters for the adsorption system are discussed further below.

2.2. METHODS

2.2.1. Preparation of NaOH-modified *Carica papaya* seed adsorbent

Carica papaya seeds from fresh ripe fruit were collected from a local farm, washed with distilled water and air-dried for 7 days. The dried seeds were ground into powder and stored in a sealed container as raw *Carica papaya* seed (RCPS). A 30 g portion of RCPS powder was weighed into a beaker and soaked in 300 mL of 0.1 M NaOH for 24 h, modifying the method of Ref. [9]. The treated RCPS was filtered, washed several times with distilled water until neutral pH was obtained, and dried in an oven at 75 °C for 24 h. The treated sample was stored as base-modified *Carica papaya* seed (BCPS).

2.2.2. Characterization of the adsorbent

The adsorbents prepared were characterized using Fourier transform infrared spectroscopy, scanning electron microscopy [10] and pH point of zero charge. A 0.15 g portion of BCPS was added to each of eleven 100 mL conical flasks containing 45 mL of 0.01 M NaCl, the pH of which was adjusted from 2 to 10 by adding 0.01 M HCl or NaOH. The total volume in each flask was made up to 50 mL by adding 0.01 M NaCl solution. The conical flasks were sealed and placed in a shaker for 12 h. The contents of the flasks were filtered, and pH was measured using a pH meter. The difference between the initial and final pH (pH_f) values, $\Delta pH = pH - pH_f$, was plotted against pH. The point of intersection of the resulting curve with the pH axis gave the PZC [11].

2.2.3. Batch adsorption study

Batch adsorption experiments were performed to investigate the influence of various adsorption parameters on the adsorption process. The adsorption parameters studied were contact time, adsorbent dose, solution pH, adsorbate concentration and temperature. The effect of contact time was determined by adding 0.1 g of BCPS to 30 mL of 50 mg/L MG and CR solutions in the single system. The solutions were shaken at 150 rpm and drawn at predetermined time intervals of 5–360 min [12]. To determine the effect of dose, 0.05–0.7 g doses of BCPS were separately added to 30 mL each of 50 mg/L CR and MG in the single system. The mixtures were agitated on a shaker at 150 rpm for 300 min at room temperature until equilibrium was attained [13]. The effect of pH on the adsorption of the two dyes by BCPS was studied by measuring 30 mL of 50 mg/L dye solutions at pH 2–11. The dye solutions were adjusted to the desired pH using 0.1 M HCl or 0.1 M NaOH. The solutions were then agitated at room temperature with 0.1 g of BCPS [14]. A 0.1 g portion of BCPS was added separately to 30 mL of different initial concentrations (10–100 mg/L) of CR and MG in single systems. The solutions were then shaken at room temperature on a shaker, with other parameters kept constant, until equilibrium was reached. To study the effect of temperature, 30 mL of 50 mg/L dye solutions in the single system were agitated with 0.1 g of BCPS at 30–60 °C in a mechanical thermostatic water-bath shaker. Shaking continued until equilibrium was attained. In all adsorption unit processes, the mixtures were filtered and analyzed for the concentrations of CR and MG left unadsorbed using a UV–Vis spectrophotometer adjusted to λ_{max} values of 496 nm for CR and 616 nm for MG [15].

2.2.4. Analytical tools

The quantities of CR and MG adsorbed by BCPS were obtained from analysis of the filtrates using a UV–Vis spectrophotometer and the mass-balance equation

$$q_e = \frac{(C_i - C_e)V}{m}, \tag{1}$$

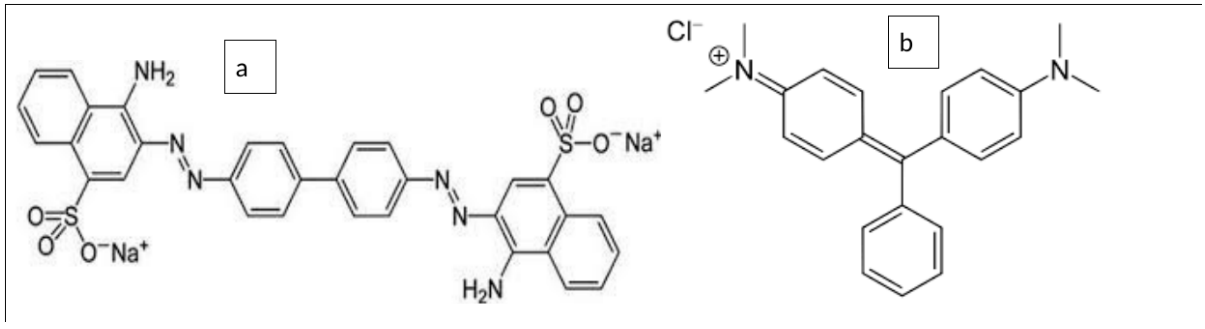

Figure 1. Molecular structures of (a) Congo red (CR) and (b) malachite green (MG).

where q_e is the quantity of dye adsorbed per unit mass of BCPS (mg/g), C_i is the initial dye concentration (mg/L), C_e is the equilibrium dye concentration (mg/L), V is the solution volume (L) and m is the BCPS mass (g).

2.2.5. Adsorption isotherm, kinetic and thermodynamic studies

The equations used for determining adsorption parameters in the isotherm, kinetic and thermodynamic studies are given in Table 1. In the table, $C_{Ae} = (C_i - C_e)$ (mg/L) is the amount of adsorbate adsorbed on the adsorbent at equilibrium, C_e (mg/L) is the amount of adsorbate in solution at equilibrium, R is the gas constant (8.314 J/mol/K), and T is temperature (K).

3. RESULTS AND DISCUSSION

3.1. PHYSICOCHEMICAL PROPERTIES OF BCPS

The results of BCPS characterization analyses are presented in Figure 2. Figure 2a shows the micrographic image of BCPS. The pores were open and free of foreign materials at the surface. Figure 2b, the image of BCPS after MG adsorption, shows a change in surface morphology with the presence of MG molecules. However, the molecules were not explicitly visible in the pores, suggesting that MG–BCPS interaction may have occurred through functional groups. The surface of BCPS after CR adsorption revealed adsorbed molecules on the pores and interstitial spaces (Figure 2c), suggesting pore adsorption.

The peak at 3341 cm^{-1} was assigned to O–H stretching vibration of hydrogen-bonded alcohol. A band at 2941 cm^{-1} can be attributed to asymmetric and symmetric C–H stretching vibration of alkane. A peak at 2461 cm^{-1} can be assigned to C–H stretching vibration of an aromatic aldehyde. After adsorption of the dyes, there were shifts in some adsorption bands. The peak observed at 3341 cm^{-1} shifted to 3362 cm^{-1} after MG adsorption, whereas a blue shift to 3281 cm^{-1} occurred after CR adsorption. The band obtained at 2942 cm^{-1} shifted to 2961 cm^{-1} after CR adsorption (Figure 2d–f).

As presented in Table 2, the BCPS functional groups involved in MG adsorption were O–H, C≡N, C≡C and C=O at 1620 cm^{-1}. O–H underwent a red shift upon MG adsorption. This suggested that an electron-donating/pushing group, probably N≡, interacted with the hydroxyl group, weakening the strength of the O–H bond. This explained the disappearance of C≡N at 2461 cm^{-1}, which appeared as a new C–N bond at 1080 cm^{-1}. The C≡C shifted to the blue region, indicating interaction with an electron-withdrawing group, probably N^+, that strengthened the bond. In addition, C=O at 1620 cm^{-1} disappeared, suggesting formation of a new C–O–C bond at 1080 cm^{-1}. O–H, C–H, C≡N, C≡C and C=O at 1620 cm^{-1} were involved in CR adsorption. The O–H bond underwent a blue shift, suggesting interaction with an electron-withdrawing group, probably S–O–Na^+. C–H may have interacted with one of the electron-rich centers on CR, leading to a red shift in the bond strength.

A graph of ΔpH against pH_i was plotted, and the pH_{pzc} value was obtained from the point where the graph crossed the x-axis such that ΔpH equaled zero (Figure 2g). The pH_{pzc} obtained for BCPS was 6.2. The pH_{pzc} value indicates the net surface charge on the adsorbent surface. According to the literature, the charge on the adsorbent surface is negative at $pH > pH_{pzc}$, whereas the surface is positively charged at $pH < pH_{pzc}$ [17, 18].

3.2. EFFECT OF EXPERIMENTAL PARAMETERS ON THE ADSORPTION OF MG AND CR

Contact time is one of the parameters that determines how economical the adsorption process is [19]. The results presented in Figure 3a,b show that the process occurred in three phases. The first phase was a rapid adsorption phase, indicated by the rapid increase in the quantity of dye adsorbed; the second phase showed less rapid adsorption; and the third phase signified attainment of equilibrium. Adsorption of MG and CR onto BCPS attained equilibrium at 180 min, with maximum adsorption capacities of 14.04 and 9.54 mg/g, respectively. Adsorbate and adsorbent chemistry may not have been responsible for adsorption efficiency here because CR has more reactive centers than MG. Therefore, MG, with smaller molecular mass, may more easily gain access into the BCPS matrix and be adsorbed compared with CR [20–22]. The molecular masses of CR and MG are 697 and 365 g/mol, respectively. MG may have easier access to the adsorbent pores; therefore, physisorption may be favored. On the other hand, CR has 12 electron-density centers compared with two in MG. Chemisorption may favor CR adsorption compared with MG, depending on adsorption-matrix pH, adsorbent functional groups, adsorbent pore size and pH_{pzc}.

The quantity of dye adsorbed per unit mass of adsorbent (q_e) decreased with increasing adsorbent dose for all systems studied. For MG adsorption by BCPS (Figure 3c,d), q_e decreased from 26.63 to 2.07 mg/g as the adsorbent dose increased from 0.05 to 0.7 g. For CR adsorption, q_e decreased with increasing BPS dose from 17.09 to 1.87 mg/g. The results imply that, at lower doses, the available adsorption sites were adequately utilized by the ad-

Table 1. Isotherm, kinetic and thermodynamic equations used in the adsorption study [16].

S/N	Model	Linear equation
Isotherm models		
1	Langmuir	$\frac{C_e}{q_e} = \frac{1}{K_L q_m} + \frac{C_e}{q_m}$
2	Freundlich	$\log q_e = \log K_F + \frac{1}{n} \log C_e$
3	Dubinin–Radushkevich	$\ln q_e = \ln q_0 - \beta\varepsilon^2$
Kinetic models		
1	Pseudo-first order	$\log(q_e - q_t) = \log q_e - \frac{k_1}{2.303} t$
2	Pseudo-second order	$\frac{t}{q_t} = \frac{1}{h} + \frac{t}{q_e}$
Thermodynamic equations		
1	Gibbs free energy	$\Delta G = -RT \ln K$
2	Enthalpy and entropy	$\log\left(\frac{C_{Ae}}{C_e}\right) = \frac{\Delta S^0}{2.303R} - \frac{\Delta H^0}{2.303RT}$

Table 2. BCPS functional groups before and after adsorption of MG and CR.

FTIR peak (cm^{-1})	Functional group	After MG adsorption (cm^{-1})	Δ peak (cm^{-1})	After CR adsorption (cm^{-1})	Δ peak (cm^{-1})
3341	O–H	3361	+20	3281	-60
2941	C–H	2941	0	2961	+20
2461	C≡N	none	–	–	–
2342	C≡C	2320	-22	2320	-22
1742	C=O	1742	0	1742	0
1682	C=C	1682	0	1682	0
1620	C=O	none	–	none	–
1422	C–C	1422	0	1422	0
–	–	1080 (C–N; C–O) new peak	–	1042 (C–N; C–O) new peak	–

sorbates, leading to higher adsorption capacity. As the adsorbent dose increased, adsorption sites increased, meaning that many adsorption sites were not adequately utilized, leading to unsaturation of the adsorbent surface and therefore lower adsorption capacity [13, 14]. The smaller molecular mass of MG compared with CR may have enhanced its adsorption.

The influence of pH on the adsorption of MG and CR onto BCPS was investigated, and the results are presented in Figure 3e,f. The optimum pH for MG adsorption was in the alkaline region, pH 9 (14.60 mg/g). The maximum CR adsorption capacity of 14.88 mg/g was achieved at pH 3. These results can be explained as follows: MG is a cationic dye with a positive charge on its surface. At pH > pH_{pzc} of BCPS (6.2), the adsorbent surfaces become negatively charged. The electrostatic interaction between the opposite charges on the sorbate and sorbent surfaces contributed to MG adsorption at alkaline pH. Similarly, the maximum q_e was obtained in the acidic region for CR adsorption due to electrostatic attraction between the negative surface of CR and the positive adsorbent surfaces at pH < pH_{pzc} [23, 24]. The pH of the mixture induced a driving force that enhanced BCPS uptake of CR and MG. BCPS had similar capacities for both adsorbates.

3.3. EQUILIBRIUM ISOTHERM STUDY

3.3.1. Effect of initial concentration and mixture matrix on adsorption capacity of BCPS for MG and CR in single and binary systems

Concentration is one of the major driving forces determining transfer of adsorbate to the adsorbent surface. As shown in Figure 4, the quantity of dye adsorbed per unit mass of adsorbent (q_e) increased as the initial dye concentration increased from 20 to 100 mg/L in both the single and binary solutions. In Figure 4a,b, q_e increased from 5.55 to 25.54 mg/g and from 3.35 to 25.33 mg/g for the single and binary systems, respectively. Similarly, for CR adsorption, q_e increased from 3.50 to 6.46 mg/g and from 2.24 to 22.42 mg/g for the single and binary systems, respectively (Figure 4c,d).

The BCPS capacity (q_m) for MG adsorption was 42.37 and 7.62 mg/g in the single and binary systems, respectively, while for CR adsorption in the single and binary systems, the q_m values were 6.95 and 5.58 mg/g, respectively (Tables 3 and 4). The presence of another dye had an antagonistic effect on MG and CR adsorption, as reflected in the q_m values obtained for both systems. A similar effect was reported for the adsorption of crys-

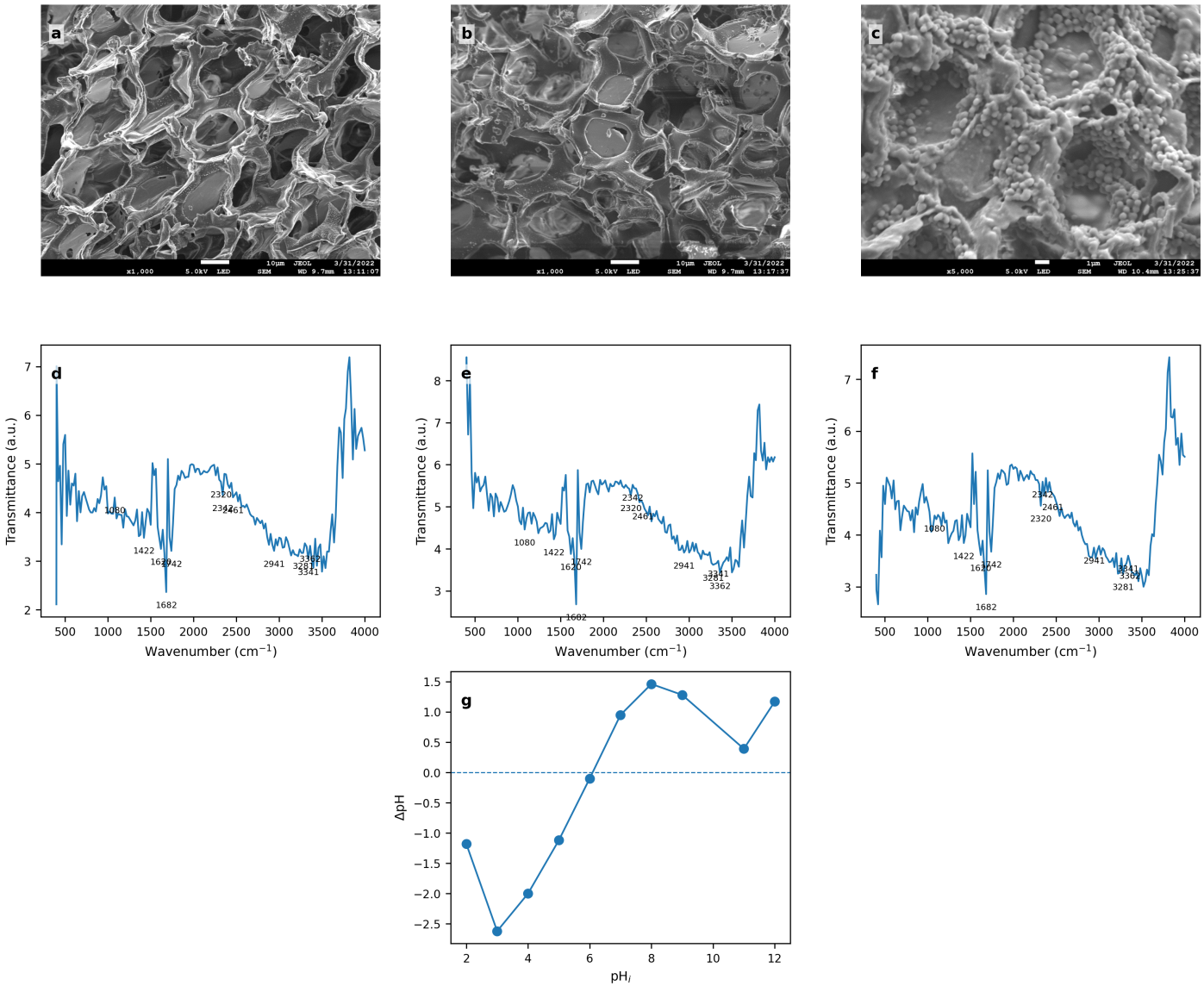

Figure 2. BCPS SEM before adsorption (a); BCPS SEM after MG adsorption (b); BCPS SEM after CR adsorption (c); BCPS FTIR before adsorption (d); BCPS FTIR after MG adsorption (e); BCPS FTIR after CR adsorption (f); pH$_{pzc}$ of BCPS (g).

tal violet and malachite green dyes. In addition, for all systems studied, the values of dimensionless separation factor (R_L) were less than unity, indicating favorable adsorption. The 1/n values obtained from the Freundlich model were less than 1 for single systems and greater than 1 for binary systems, indicating cooperative adsorption in binary systems. This information may be useful when characterizing the complexity of an unknown adsorption matrix. Considering the regression-coefficient (R^2) values, the adsorption of CR in single and binary systems onto BCPS followed the Langmuir isotherm model, confirming monolayer adsorption on homogeneous surfaces. MG adsorption in the single system fitted better to the Temkin isotherm model, which assumes a linear decrease in adsorption energy with coverage. The results also revealed that the Dubinin–Radushkevich model better explained MG adsorption in the binary system, with mean free energy (E) values less than 8 kJ/mol, which may indicate physisorption. Similar results have been reported [25–29].

3.4. ADSORPTION KINETIC STUDY

The results in Figure 5a,b show that the quantity of MG adsorbed per unit mass of adsorbent decreased from 14.20 to 13.74 mg/g with increasing temperature in the single system, whereas q_e increased from 10.57 to 12.71 mg/g in the binary system. CR adsorption showed an increase in q_e as temperature increased for both single and binary systems (Figure 5c,d). These results indicate that BCPS adsorptive pores were large enough for MG accessibility at ambient temperature. Increasing temperature enhanced adsorbate-molecule kinetic energy, reduced bulk-solution viscosity and desorbed already adsorbed MG. However, MG in the binary solution, CR in the single system and CR in the binary system were bulky and suspected to be larger than the average BCPS pore diameter. Increasing temperature increased adsorbate-molecule kinetics and may also have softened the pore openings, leading to molecular knocking. The higher the temperature, the higher the driving force and the more molecules were

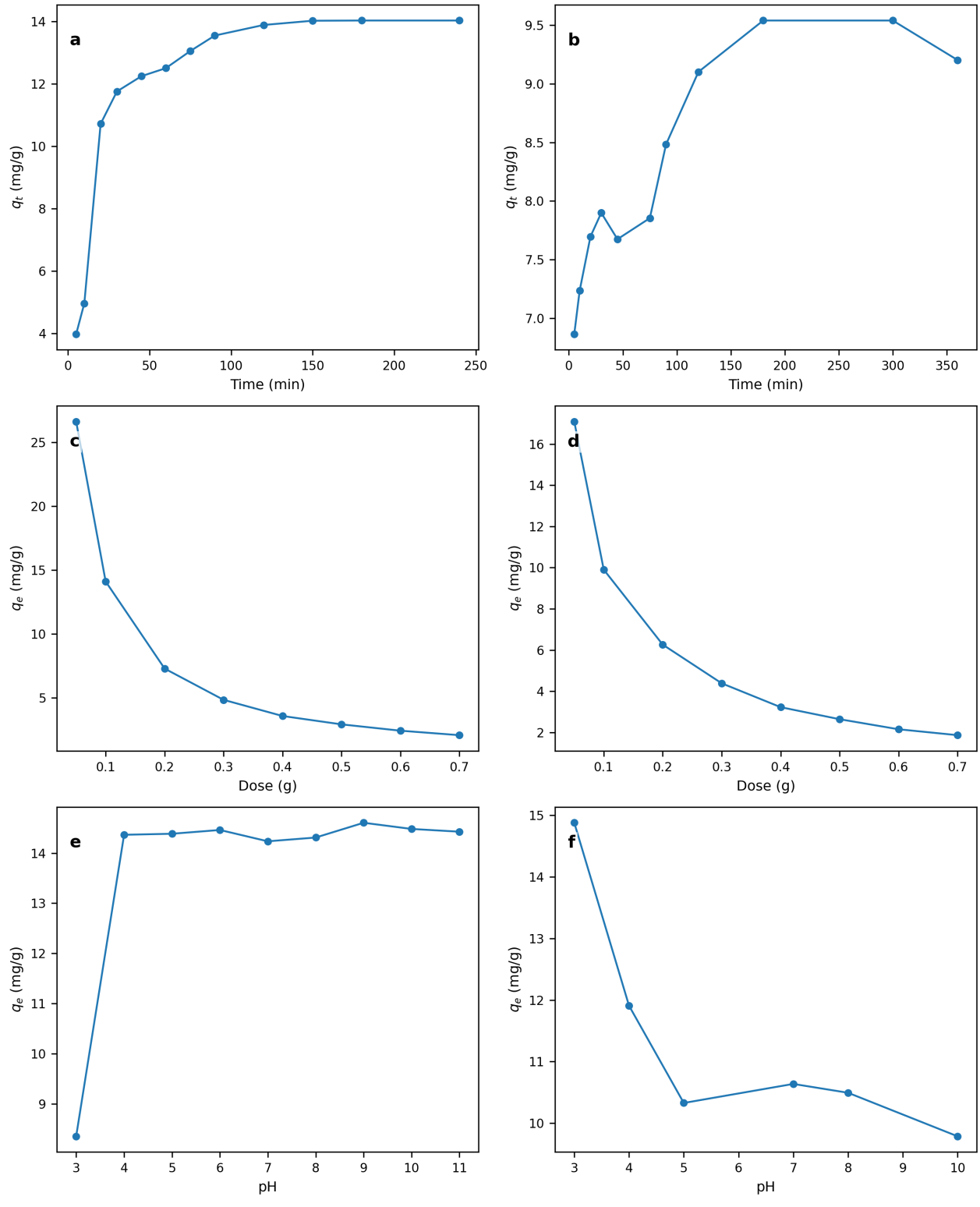

Figure 3. Effect of contact time on MG adsorption onto BCPS (a); effect of contact time on CR adsorption onto BCPS (b); effect of BCPS dose on MG adsorption (c); effect of BCPS dose on CR adsorption (d); effect of pH on MG adsorption onto BCPS (e); effect of pH on CR adsorption onto BCPS (f).

forced into the pores [44, 45].

The R^2 values for pseudo-second-order kinetics obtained for MG and CR adsorption were higher than those for the pseudo-first-order and Elovich kinetic models (Table 5). This indicates conformity of the adsorption process to the pseudo-second-order kinetic model, implying that the rate-limiting step is chemisorption [46]. Further confirmation is provided by the agreement between calculated adsorption capacities, q_e (calc), for the pseudo-second-order model and the experimental adsorption capacities, q_e (expt). Similar observations have been reported [47, 48].

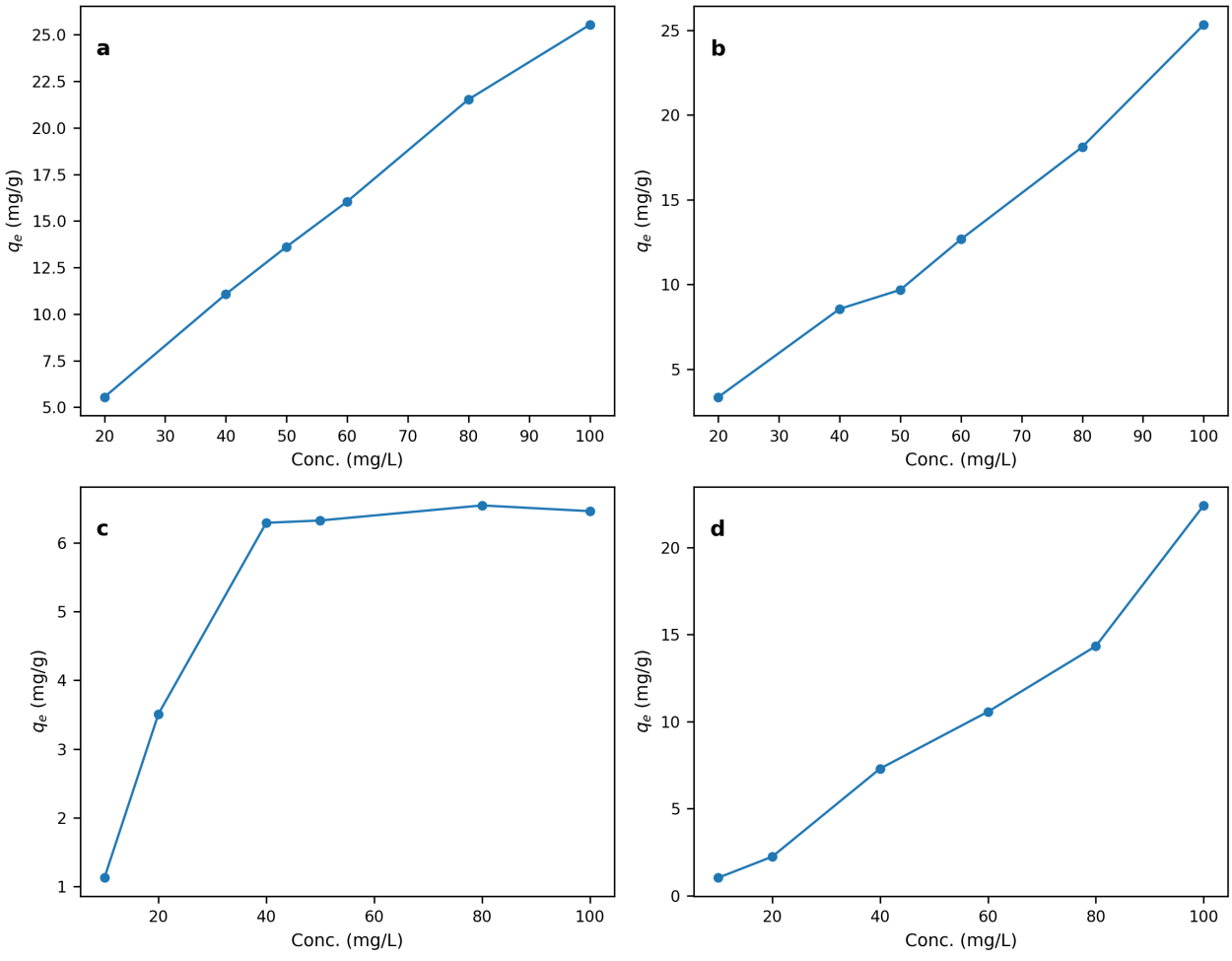

Figure 4. Effect of initial MG concentration on its adsorption onto BCPS in the single system (a); MG onto BCPS in the binary system (b); CR onto BCPS in the single system (c); CR onto BCPS in the binary system (d).

Table 3. Isotherm parameters for adsorption of MG and CR onto BCPS in single and binary systems.

Models/parameters	MG		CR	
	Single	Binary	Single	Binary
Langmuir				
R^2	0.9603	0.8915	0.9918	0.9357
q_m (mg/g)	42.37	7.62	6.95	5.58
K_a (mg/g)	0.106	0.0342	0.206	0.0238
R_L	0.16	0.37	0.088	0.46
Freundlich				
R^2	0.9666	0.9388	0.7838	0.9319
K_f (mg/g)(L/g)^n	4.715	0.0505	2.0592	0.0397
$1/n$	0.6685	1.9121	0.308	1.7325
Dubinin–Radushkevich				
R^2	0.8806	0.9657	0.9485	0.9341
β (mol^2/J^2)	8×10^{-7}	3×10^{-5}	1×10^{-5}	5×10^{-5}
q_0 (mg/g)	20.06	24.99	6.94	20.39
E (kJ/mol)	0.7906	0.1291	0.2236	0.1
Temkin				
R^2	0.9700	0.8268	0.8517	0.9051
A_T (L/g)	1.138	0.172	0.497	0.143
b_T (J/mol)	283.77	245.55	1286.39	293.41

Table 4. Comparison of maximum adsorption capacities (q_m) of BCPS with other adsorbents.

Adsorbent	Adsorbate	q_m (mg/g) single system	q_m (mg/g) binary system	Reference
Banana peel powder	Congo red	1.721	–	[30]
Native fungal biomass	Congo red	90.4	–	[31]
Tunics of the corm of saffron	Congo red	6.2	–	[32]
Cymbopogon winterianus	Congo red	3.5	–	[33]
Burned shoot of *E. crassipes*	Congo red	5.16	–	[34]
Amino-grafted biochar	Congo red	89.3	–	[35]
Gum ghatti–acrylamide grafted copolymer coated with zero-valent iron	Congo red	153.3	–	[36]
BCPS	Congo red	6.95	5.58	Present study
Coconut shell	Malachite green	61.83	–	[37]
Azadirachta indica leaf	Malachite green	7.65	–	[38]
Lignin	Malachite green	31.2	–	[39]
Walnut shell	Malachite green	11.76	–	[40]
Catha edulis stem	Malachite green	5.62	–	[41]
Lupinus albus seed peel	Malachite green	20.90	–	[42]
Coal-associated soil	Malachite green	89.97	–	[43]
BCPS	Malachite green	42.37	7.62	Present study

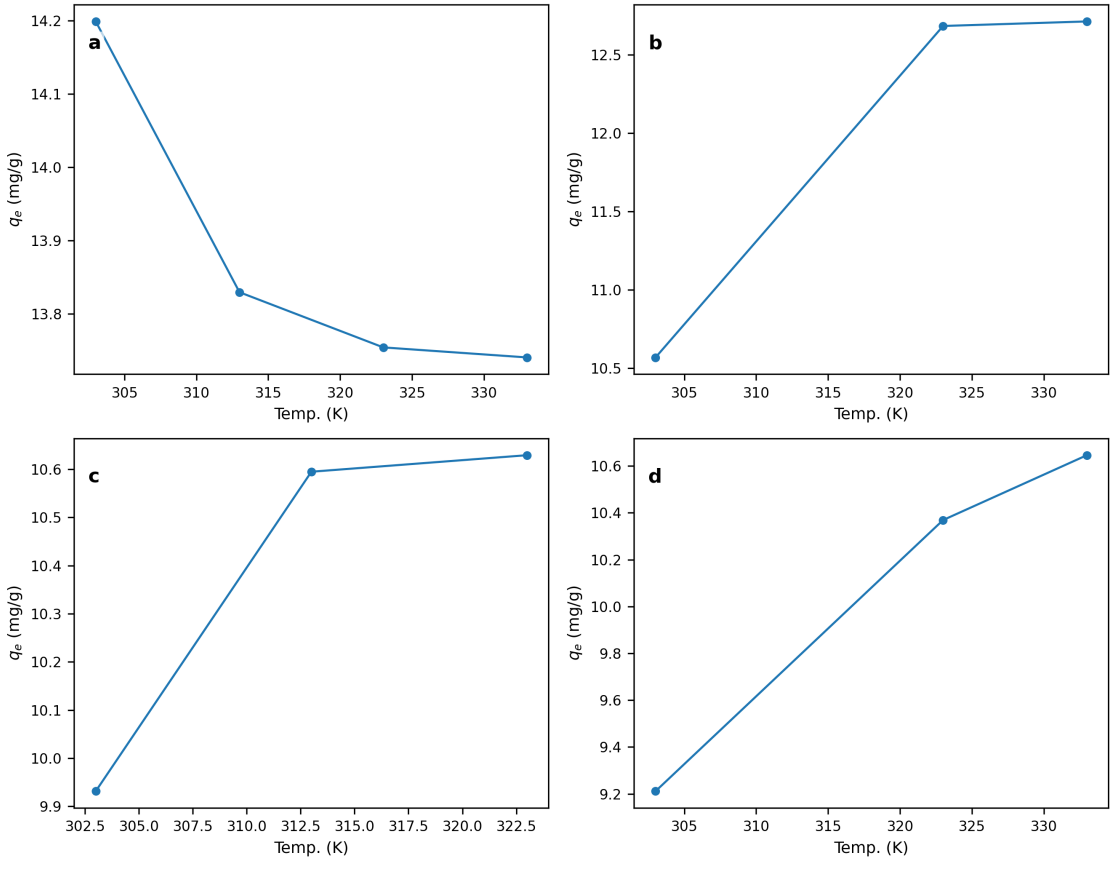

Figure 5. Effect of temperature on MG adsorption onto BCPS in the single system (a); MG onto BCPS in the binary system (b); CR onto BCPS in the single system (c); CR onto BCPS in the binary system (d).

Table 5. Kinetic parameters for adsorption of MG and CR onto BCPS.

Model/parameter	MG	CR
q_e (expt) (mg/g)	14.035	9.539
Pseudo-first order		
R^2	0.8903	0.4407
q_e (calc) (mg/g)	36.521	2.011
k_1 (min^{-1})	0.0665	0.0029
Pseudo-second order		
R^2	0.9977	0.9289
q_e (calc) (mg/g)	14.925	9.881
k_2 (g/mg min)	5.912×10^{-3}	9.17×10^{-4}
Elovich		
R^2	0.8669	0.8439
α (mg/g min)	3.641	940.345
β (g/mg)	0.3675	1.3217

Table 6. Thermodynamic parameters for adsorption of MG and CR in single and binary systems by BCPS.

	Temperature (K)			
System/parameter	303	313	323	333
MG, single system				
ΔG (kJ mol^{-1})	-3.28	-3.27	-3.26	-3.25
ΔH (kJ mol^{-1})	-3.48	–	–	–
ΔS (J mol^{-1} K^{-1})	-0.67	–	–	–
MG, binary system				
ΔG (kJ mol^{-1})	-49.90	-50.71	-51.52	-52.34
ΔH (kJ mol^{-1})	-25.31	–	–	–
ΔS (J mol^{-1} K^{-1})	+81.16	–	–	–
CR, single system				
ΔG (kJ mol^{-1})	-16.48	-16.73	-16.98	-17.23
ΔH (kJ mol^{-1})	-8.87	–	–	–
ΔS (J mol^{-1} K^{-1})	+25.11	–	–	–
CR, binary system				
ΔG (kJ mol^{-1})	-22.80	-23.15	-23.49	-23.84
ΔH (kJ mol^{-1})	-12.32	–	–	–
ΔS (J mol^{-1} K^{-1})	+34.59	–	–	–

3.5. THERMODYNAMIC STUDIES

Temperature is an important factor that affects the adsorption process because it determines process feasibility. The thermodynamic parameters (ΔG, ΔH and ΔS) for MG and CR adsorption were obtained from the slope and intercept of the plot of $\ln K_o$ against inverse temperature, $1/T$. From the thermodynamic-study results presented in Table 6, adsorption of MG and CR by BCPS in single and binary systems was exothermic because all ΔH values were negative. The feasibility and spontaneity of the adsorption process were further verified from the negative ΔG values obtained. A lower degree of disorderliness at the sorbate/sorbent interphase was observed for MG adsorption in the single system, as reflected in the negative ΔS value. However, ΔS values were positive for MG adsorption in the binary system and CR adsorption in both systems. Similar results have been reported [49–51].

4. CONCLUSION

The study showed that increasing temperature enhanced adsorption of the adsorbate with higher molecular mass (Congo red) and adsorption in binary systems (bulky matrix), whereas it reduced adsorption of the adsorbate with lower molecular mass (malachite green). In addition, $1/n$ values obtained from the Freundlich model were below unity for single systems and above unity for binary systems. This information can be useful, considering adsorbate molecular mass, adsorbent pore profile and adsorption matrix, in developing selective adsorbents for specific adsorption processes. Further studies may develop a molecular-mass–pore-size adsorption model.

DATA AVAILABILITY

The data will be available on request from the corresponding author.

References

[1] S. A. Adesokan, A. A. Giwa & I. A. Bello, "Environmental, health and economic implications of emerging contaminants in Nigeria environment", Journal of the Nigerian Society of Physical Sciences **4** (2022) 842. https://doi.org/10.46481/jnsps.2022.842.

[2] A. Chan, Rubiyatno & Z. Akhmetov, "Environmental impact of synthetic dyes on groundwater in Malaysia: sources, distribution, transport mechanisms, and mitigation strategies", Tropical Aquatic and Soil Pollution **4** (2024) 87. https://doi.org/10.53623/tasp.v4i2.476.

[3] M. Abewaa, A. Mengistu, T. Takele, J. Fito & T. Nkambule, "Adsorptive removal of malachite green dye from aqueous solution using *Rumex abyssinicus*-derived activated carbon", Scientific Reports **13** (2023) 14701. https://doi.org/10.1038/s41598-023-41957-x.

[4] Q. Hu & L. Hao, "Adsorption technologies in wastewater treatment processes", Water **17** (2025) 2335. https://doi.org/10.3390/w17152335.

[5] J. O. Adinde, O. Ugwuanyi-Nnadi, O. J. Uche & U. J. Anieke, "Evaluation and selection of pawpaw accessions for production and breeding programmes in Southeast Nigeria using Rank Summation Index (RSI) approach", Journal of Agricultural Science and Practice **9** (2024) 157. https://doi.org/10.31248/JASP2024.484.

[6] Y. Liu, B. Biswas & R. Naidu, "Novel adsorbents for environmental remediation", Processes **12** (2024) 670. https://doi.org/10.3390/pr12040670.

[7] A. Anjum, S. A. Mazari, Z. Hashmi, A. S. Jatoi, R. Abro, A. W. Bhutto, N. M. Mubarak, M. H. Dehghani, R. R. Karri, A. H. Mahvi & S. Nasseri, "A review of novel green adsorbents as a sustainable alternative for the remediation of chromium(VI) from water environments", Heliyon **9** (2023) e15575. https://doi.org/10.1016/j.heliyon.2023.e15575.

[8] B. Alawa, S. Singh, S. Chakma, R. Kishor, C. S. Lundborg & V. Diwan, "Development of novel biochar adsorbent using agricultural waste biomass for enhanced removal of ciprofloxacin from water: insights into the isotherm, kinetics, and thermodynamic analysis", Chemosphere **375** (2025) 144252. https://doi.org/10.1016/j.chemosphere.2025.144252.

[9] N. D. Shooto & E. B. Naidoo, "Detoxification of wastewater by pawpaw (*Carica papaya* L.) seed adsorbents", Asian Journal of Chemistry **31** (2019) 2249. https://doi.org/10.14233/ajchem.2019.22051.

[10] A. Abdullah & A. Mohammed, "Scanning electron microscope (SEM): a review", Proceedings of the 2018 International Conference on Hydraulic and Pneumatics, Baile Govora, Romania, 7–9 November (2018) 77. Available online: https://fluidas.ro/hervex/proceedings2018/77-85.pdf.

[11] S. Muzaffar & H. Tahir, "Enhanced synthesis of silver nanoparticles by combination of plant extract and starch for the removal of cationic dye from simulated wastewater using response surface methodology", Journal of Molecular Liquids **252** (2018) 368. https://doi.org/10.1016/j.molliq.2018.01.007

[12] K. S. Baidya & K. Kumar, "Adsorption of brilliant green dye from aqueous

solution onto chemically modified areca nut husk'', South African Journal of Chemical Engineering **35** (2021) 33. https://doi.org/10.1016/j.sajce.2020.11.001

[13] A. A. Giwa, S. A. Adesokan & I. A. Bello, ''Adsorption of pyrimethamine from wastewater using activated carbons prepared from *Daniellia-oliveri* sawdust'', International Journal of Environmental Analytical Chemistry **103** (2021) 1938. https://doi.org/10.1080/03067319.2021.1884858.

[14] A. A. Giwa, I. A. Bello, M. A. Oladipo & D. O. Aderibigbe, ''Competitive adsorption of Congo red in single and binary systems using a low-cost adsorbent'', Journal of Health and Pollution **11** (2021) 210912. https://doi.org/10.5696/2156-9614-11.31.210912.

[15] O. S. Bello, O. C. Alao, T. C. Alagbada & A. M. Olatunde, ''Biosorption of ibuprofen using functionalized bean husks'', Sustainable Chemistry and Pharmacy **13** (2019) 100151. https://doi.org/10.1016/j.scp.2019.100151.

[16] S. A. Adesokan, A. A. Giwa & I. A. Bello, ''Adsorptive removal of ibuprofen from waste stream using sawdust-based adsorbents'', International Journal of Engineering Research in Africa **55** (2021) 172. https://doi.org/10.4028/www.scientific.net/jera.55.172.

[17] A. Osman & D. Kilic, ''Bioremoval of reactive dye Remazol Navy by Kefir grains'', Applied Biological Chemistry **62** (2019) 22. https://doi.org/10.1186/s13765-019-0429-1.

[18] A. Othmani, A. Kesraoui, R. Boada, M. Seffen & M. Valiente, ''Textile wastewater purification using an elaborated biosorbent hybrid material (luffa-cylindrica–zinc oxide) assisted by alternating current'', Water **11** (2019) 1326. https://doi.org/10.3390/w11071326.

[19] U. Yunusa, B. Usman & M. B. Ibrahim, ''Experimental and quantum chemical investigation for the single and competitive adsorption of cationic dyes onto activated carbon'', Algerian Journal of Engineering and Technology **4** (2021) 7. https://doi.org/10.5281/zenodo.4504565.

[20] O. Lacin, A. Haghighatnia, F. Demir & F. Sevim, ''Adsorption characteristics and behaviors of natural red clay for removal of BY28 from aqueous solutions'', International Journal of Trend in Scientific Research and Development **3** (2019) 1037. Available online: https://paper.researchbib.com/view/paper/211235.

[21] D. Balarak, A. H. Mahvi, S. Shahbaksh, M. A. Wahab & A. Abdala, ''Adsorptive removal of azithromycin antibiotic from aqueous solution by *Azolla filiculoides*-based activated porous carbon'', Nanomaterials **11** (2021) 3281. https://doi.org/10.3390/nano11123281.

[22] E. Kavci, J. Erkmen & M. S. Bingöl, ''Removal of methylene blue dye from aqueous solution using citric-acid-modified apricot stone'', Chemical Engineering Communications **210** (2023) 165. https://doi.org/10.1080/00986445.2021.2009812.

[23] L. S. Maia, A. I. C. da Silva, E. S. Carneiro, F. M. Monticelli, F. R. Pinhati & D. R. Mulinari, ''Activated carbon from palm fibres used as an adsorbent for methylene blue removal'', Journal of Polymers and the Environment **29** (2021) 1162. https://doi.org/10.1007/s10924-020-01951-0.

[24] M. Bounaas, A. Bouguettoucha, D. Chebli, J. M. Gatica & H. Vidal, ''Role of the wild carob as biosorbent and as precursor of a new high-surface-area activated carbon for the adsorption of methylene blue'', Arabian Journal for Science and Engineering **46** (2021) 325. https://doi.org/10.1007/s13369-020-04739-5.

[25] A. Yildirim & Y. Bulut, ''Adsorption behaviors of malachite green by using crosslinked chitosan/polyacrylic acid/bentonite composites with different ratios'', Environmental Technology & Innovation **17** (2020) 100560. https://doi.org/10.1016/j.eti.2019.100560.

[26] T. Bayram, S. Bucak & D. Ozturk, ''BR13 dye removal using sodium dodecyl sulfate modified montmorillonite: equilibrium, thermodynamic, kinetic and reusability studies'', Chemical Engineering and Processing: Process Intensification **158** (2020) 108186. https://doi.org/10.1016/j.cep.2020.108186.

[27] E. Alver, A. U. Metin & F. Brouers, ''Methylene blue adsorption on magnetic alginate/rice husk bio-composite'', International Journal of Biological Macromolecules **154** (2020) 104. https://doi.org/10.1016/j.ijbiomac.2020.02.330.

[28] P. Zhang, D. O'Connor, Y. Wang, L. Jiang, T. Xia, L. Wang, D. L. Tsang, Y. S. Ok & D. Hou, ''A green biochar/iron oxide composite for methylene blue removal'', Journal of Hazardous Materials **384** (2020) 121286. https://doi.org/10.1016/j.jhazmat.2019.121286.

[29] W. M. Alghamdi & I. El Mannoubi, ''Investigation of seeds and peels of *Citrullus colocynthis* as efficient natural adsorbent for methylene blue dye'', Processes **9** (2021) 1279. https://doi.org/10.3390/pr9081279.

[30] N. K. Mondal & S. Kar, ''Potentiality of banana peel for removal of Congo red dye from aqueous solution: isotherm, kinetics and thermodynamics studies'', Applied Water Science **8** (2018) 157. https://doi.org/10.1007/s13201-018-0811-x.

[31] G. Bayramoglu & M. Y. Arica, ''Adsorption of Congo red dye by native amine and carboxyl modified biomass of *Funalia trogii*: isotherms, kinetics and thermodynamic mechanisms'', Korean Journal of Chemical Engineering **35** (2018) 1303. https://doi.org/10.1007/s11814-018-0033-9.

[32] A. Dbik, S. Bentahar, M. El Khomri, N. El Messaoudi & A. Lacherai, ''Adsorption of Congo red dye from aqueous solutions using tunics of the corm of the saffron'', Materials Today: Proceedings **22** (2020) 134. https://doi.org/10.1016/j.matpr.2019.08.148.

[33] A. Saha, B. B. Basak & M. Ponnuchamy, ''Performance of activated carbon derived from *Cymbopogon winterianus* distillation waste for scavenging of aqueous toxic anionic dye Congo red: comparison with commercial activated carbon'', Separation Science and Technology **33** (2019) 1970. https://doi.org/10.1080/01496395.2019.1620277.

[34] T. T. Roy & N. K. Mondal, ''Potentiality of *Eichhornia* shoots ash towards removal of Congo red from aqueous solution: isotherms, kinetics, thermodynamics and optimization studies'', Groundwater for Sustainable Development **9** (2019) 100269. https://doi.org/10.1016/j.gsd.2019.100269.

[35] D. J. Faheem, J. Bao, M. A. Hassan, S. Irshad & M. A. Talib, ''Multifunctional biochar novel surface chemistry for efficient capture of anionic Congo red dye: behaviour and mechanism'', Arabian Journal for Science and Engineering **44** (2019) 10127. https://doi.org/10.1007/s13369-019-04194-x.

[36] G. S. M. Reddy, M. Bhaumik & A. Maity, ''Removal of Congo red from aqueous solution by adsorption using gum ghatti and acrylamide graft copolymer coated with zero-valent iron'', International Journal of Biological Macromolecules **149** (2020) 21. https://doi.org/10.1016/j.ijbiomac.2020.01.099.

[37] S. A. H. Azaman, A. Afandi, B. H. Hameed & A. T. Mohd Din, ''Removal of malachite green from aqueous phase using coconut shell activated carbon: adsorption, desorption, and reusability studies'', Journal of Applied Science and Engineering **21** (2018) 317. https://www.researchgate.net/publication/328694563_Removal_of_malachite_green_from_aqueous_phase_using_coconut_shell_activated_carbon_Adsorption_desorption_and_reusability_studies.

[38] S. A. Odoemelam, U. N. Emeh & N. O. Eddy, ''Experimental and computational chemistry studies on the removal of methylene blue and malachite green dyes from aqueous solution by neem (*Azadirachta indica*) leaves'', Journal of Taibah University for Science **12** (2018) 255. https://doi.org/10.1080/16583655.2018.1465725.

[39] S. L. Lee, J. H. Park, S. H. Kim, S. W. Kang, J. S. Cho, J. R. Jeon, Y. B. Lee & D. C. Seo, ''Sorption behavior of malachite green onto pristine lignin to evaluate the possibility as a dye adsorbent by lignin'', Applied Biological Chemistry **62** (2019) 37. https://doi.org/10.1186/s13765-019-0444-2.

[40] S. Hajialigol & S. Masoum, ''Optimization of biosorption potential of nano biomass derived from walnut shell for the removal of malachite green from liquid solution: experimental design approaches'', Journal of Molecular Liquids **286** (2021) 110904. https://doi.org/10.1016/j.molliq.2019.110904.

[41] G. Y. Abate, A. N. Alene, A. T. Habte & D. M. Getahun, ''Adsorptive removal of malachite green dye from aqueous solution onto activated carbon of *Catha edulis* stem as a low-cost bio-adsorbent'', Environmental Systems Research **9** (2020) 29. https://doi.org/10.1186/s40068-020-00191-4.

[42] A. N. Alene, G. Y. Abate, A. T. Habte & D. M. Getahun, ''Utilization of a novel low-cost gibto (*Lupinus albus*) seed peel waste for the removal of malachite green dye: equilibrium, kinetic, and thermodynamic studies'', Journal of Chemistry (2021) 6618510. https://doi.org/10.1155/2021/6618510.

[43] T. R. Sundararaman, A. Saravanan, P. S. Kumar, M. M. Mabel, R. V. Hemavathy, S. Karishma, S. Jeevanantham, R. Hemavathi, A. Ishwariya & Kowsalya, ''Adsorptive removal of malachite green dye onto coal-associated soil and conditions optimization'', Adsorption Science & Technology (2021) 5545683. https://doi.org/10.1155/2021/5545683.

[44] N. Razmara, H. Namarvari & J. R. Meneghini, ''A new correlation for viscosity of model water–carbon nanotube nanofluids: molecular dynamics simulation'', Journal of Molecular Liquids **293** (2019) 111438. https://doi.org/10.1016/j.molliq.2019.111438.

[45] L. Loulidi, F. Boukhlifi, M. Ouchabi, A. Amar, M. Jabri, A. Kali, S. Chraibi & H. Aziz, ''Adsorption of crystal violet onto an agricultural waste residue: kinetics, isotherm, thermodynamics, and mechanism of adsorption'', Scientific World Journal **2020** (2020) 5873521. https://doi.org/10.1155/2020/5873521.

[46] E. A. Khan, Shahjahan & T. A. Khan, ''Synthesis of magnetic iron–

manganese oxide coated graphene oxide and its application for adsorptive removal of basic dyes from aqueous solution: isotherm, kinetics, and thermodynamic studies'', Environmental Progress & Sustainable Energy **38** (2019) S214. https://doi.org/10.1002/ep.12974.

[47] H. A. Chanzu, J. M. Onyari & P. M. Shiundu, ''Brewers' spent grain in adsorption of aqueous Congo red and malachite green dyes: batch and continuous flow systems'', Journal of Hazardous Materials **380** (2019) 120897. https://doi.org/10.1016/j.jhazmat.2019.120897.

[48] L. Lin, S. Tang, X. Wang, X. Sun & A. Yu, ''Adsorption of malachite green from aqueous solution by nylon microplastics: reaction mechanism and the optimum conditions by response surface methodology'', Process Safety and Environmental Protection **140** (2020) 339. https://doi.org/10.1016/j.psep.2020.05.019.

[49] T. Altun, ''Chitosan-coated sour cherry kernel shell beads: an adsorbent for removal of Cr(VI) from acidic solutions'', Journal of Analytical Science and Technology **10** (2019) 14. https://doi.org/10.1186/s40543-019-0172-6.

[50] Z. Bingul, ''The use of waste green tea leaves for crystal violet adsorption: kinetic and thermodynamic studies'', Journal of the Institute of Science and Technology **11** (2021) 2645. https://www.researchgate.net/publication/357084040_The_Use_of_Waste_Green_Tea_Leaves_for_Crystal_Viyole_Adsorption_Kinetic_Equilibrium_and_Thermodynamics_Studies1003271-2004279.

[51] J. Sheeja, K. Sampath & R. Kesavasamy, ''Experimental investigations on adsorption of reactive toxic dyes using *Hedyotis umbellate* activated carbon'', Adsorption Science & Technology **2021** (2021) 5035539. https://doi.org/10.1155/2021/5035539.